

<sup>4</sup> A. G. Chynoweth and A. A. Murray, *Phys. Rev.* **123**, 515 (1961).

<sup>5</sup> M. Glicksman and R. A. Powlus, *Phys. Rev.* **121**, 1659 (1961).

<sup>6</sup> B. D. Osipov and A. N. Khvoshchev, *Zh. Eksperim. i Teor. Fiz.* **43**, 1179 (1962) [*Soviet Phys. JETP* **16**, 833 (1963)].

<sup>7</sup> B. Ancker-Johnson, in *Proceedings of the International Conference on Physics of Semiconductors, Exeter* (The Institute of Physics and the Physical Society, London, 1962), p. 131.

<sup>8</sup> M. Toda, *Japan. J. Appl. Phys.* **2**, 467 (1963).

<sup>9</sup> B. Ancker-Johnson, *Phys. Rev. Letters* **9**, 485 (1962).

<sup>10</sup> B. B. Kadomtsev, in *Reviews of Plasma Physics*, **2**, edited by Acad. M. A. Leontovich (Consultants Bureau, New York, 1966), p. 153.

<sup>11</sup> C. Hilsun and A. C. Rose-Innes, *Semiconducting III-V Compounds* (Pergamon, New York, 1961), p. 126.

<sup>12</sup> L. V. Dubovoi and V. G. Shanskii, *Zh. Eksperim. i Teor. Fiz.* **56**, 766 (1969) [*Soviet Phys. JETP* **29**, 416 (1969)].

<sup>13</sup> W. S. Chen and B. Ancker-Johnson, in *Proceedings of the Conference on Pulsed, High-Density Plasmas*, Los Alamos, 1967 (unpublished); *Bull. Am. Phys. Soc.* **12**, 712 (1967); A. P. Shotov, S. P. Grishechkina, and R. A. Muminov, *Zh. Eksperim. i Teor. Fiz.* **52**, 71, (1967) [*Soviet Phys. JETP* **25**, 45 (1967)].

<sup>14</sup> W. S. Chen and B. Ancker-Johnson, *Appl. Phys. Letters* **15**, 59 (1969).

<sup>15</sup> K. Ando and M. Glicksman, *Phys. Rev.* **154**, 316 (1967).

## Ettingshausen Effect in the Intermediate State of Thin Superconducting Pb Films\*

V. A. ROWE AND R. P. HUEBENER

*Argonne National Laboratory, Argonne, Illinois 60439*

(Received 1 June 1970)

Earlier measurements of the Nernst effect in thin films of Pb, Sn, and In have shown that below a critical film thickness  $d_c$ , the entropy per unit length and per unit flux transported by the vortices decreases strongly with decreasing film thickness. To check this behavior, we have measured the Ettingshausen effect in the intermediate state of superconducting Pb films at 4.2 K as a function of the magnetic field. The films investigated were 0.75 and 3.16  $\mu\text{m}$  thick. The Ettingshausen data clearly confirm the earlier results obtained from the Nernst effect. It is suggested that the decrease of the transport entropy with decreasing film thickness, found below  $d_c$ , is due to the increasing vortex interaction present in very thin type-I films.

### I. INTRODUCTION

There is now an impressive body of evidence, theoretical<sup>1-3</sup> and experimental,<sup>4-6</sup> indicating the presence of a vortex state in thin superconducting type-I films that is distinctly different from the usual intermediate state found in thick films and foils and in bulk material. Magnetization experiments<sup>5</sup> demonstrate that in the case of Pb films at 4.2 K, the new state is established in films thinner than a critical thickness  $d_c$  of about 1.5  $\mu\text{m}$ .

Previous thermomagnetic experiments<sup>7</sup> on thin films of Pb and on Sn and In using the Nernst effect showed that  $S_\phi/\phi$ , the entropy per unit length and per unit flux transported by the vortices, as a function of film thickness passes through a maximum between 3 and 7  $\mu\text{m}$ , depending on the material, and diminishes in the thinnest films investigated. This behavior of the transport entropy for small film thickness had been explained tentatively by the increasing vortex interaction present in thin type-I films. However, the Nernst-effect measurements may be complicated by the fact that relatively large temperature gradients have to be employed leading to an appreciable nonuniformity of the characteristic superconducting parameters across the sample. This complication can be avoided in an experiment which measures the Ettingshausen effect.<sup>8</sup>

In order to confirm our earlier results from the Nernst effect on the transport entropy in thin type-I films, we have studied the Ettingshausen effect in Pb films of 0.75 and 3.16  $\mu\text{m}$  thickness. The Ettingshausen measurements clearly confirmed that, below a critical film thickness, the transport entropy in type-I films diminishes with decreasing film thickness.

### II. EXPERIMENTAL TECHNIQUES

Figure 1 shows schematically how the samples and the electronics were arranged for the Ettingshausen experiments. The samples were made by evaporation of 99.999% pure Pb<sup>9</sup> from a Joule-heated tantalum boat in a vacuum of  $10^{-5}$  Torr or lower. Microscope slides 1 mm thick were cut to  $3.8 \times 1.3$  cm and masked by a thin-foil shadow mask produced by photo reduction and etching techniques. Niobium potential and copper current leads were soldered with pure In to the substrate prior to the deposition. Film thickness was measured by weighing thin cover glass slides on a microbalance before and after the film deposition. The distance between heat sinks was 2.54 cm, the distance between voltage probes was 2.28 cm, and the film width was 0.96 cm. The substrates were cleaned in a three-step process: They were first scrubbed with detergent, then placed in an ultrasonic cleaner with ethyl alcohol, and

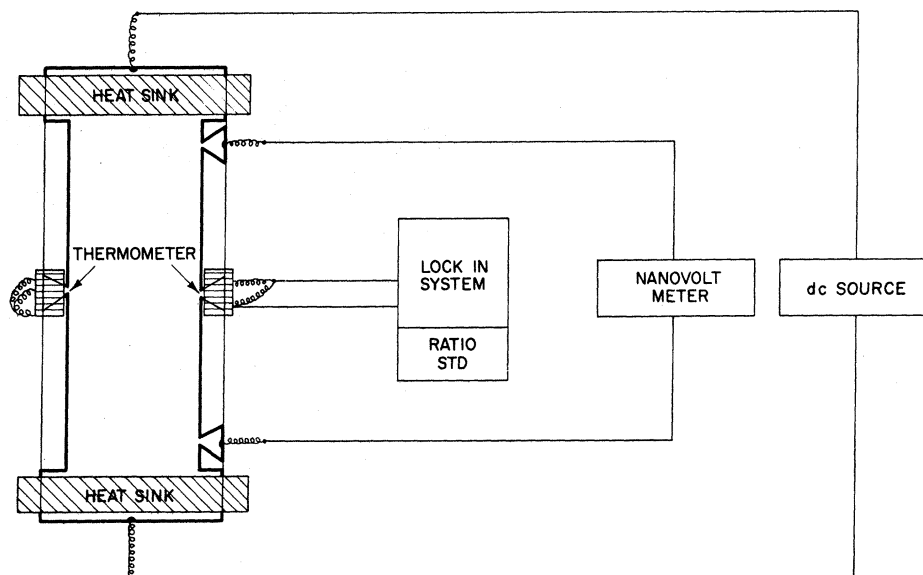


FIG. 1. Specimen geometry, including the heat sinks and thermometers, and the longitudinal current and voltage probes, together with a scheme of the electronics.

finally positioned in a vapor degreaser running on trichloroethylene. The still-hot substrates were then put in the vacuum chamber which was quickly pumped to working pressure.

Thermometers for measuring the transverse temperature gradient were prepared from 680- $\Omega$  1/10-W Allen Bradley carbon resistors by grinding to flat rectangles and in the process matching room-temperature resistances. Each ground resistor was then epoxied to a C-shaped clamp made of oxygen-free high-conductivity copper (OFHC) with Stycast 2850 GT<sup>10</sup> resin. These clamp-mounted resistors were screwed to the film-substrate sample using Apiezon N grease to aid in heat transfer, and were electrically connected via 2-mil chromel wires. The cryostat used was similar to that described in Ref. 7 except that an OFHC block was added to provide the heat sinks to the He bath in which the cryostat was immersed, as indicated in Fig. 1. One of the heat sinks was removable and a heater could be put in its place for thermal-conductivity measurements on the same specimen. During the heat-conductivity measurements, only one thermometer was used to measure the temperature gradients produced by the heat current flowing through the sample and into the bath via the remaining heat sink. The heater was a 10- $\Omega$  1/10-W Allen Bradley resistor epoxied (with E & C 2850 GT) to an OFHC block which was clamped and greased to the sample. The magnetic field was supplied by a superconducting solenoid in the Dewar. The pressure in the cryostat was typically  $5 \times 10^{-7}$  Torr (measured at the Dewar head) except during resistance measurements when exchange gas was employed.

Referring to Fig. 1, the sample current is derived from a well-regulated current supply, and the resultant voltage drop along the sample is measured with a nanovoltmeter. The two thermometers form two arms of an ac Wheatstone bridge, while the variable arms are incorporated in a Gertsch ratio standard transformer. A PAR model HR-8 lock-in amplifier supplies the driving current for the bridge and detects the out-of-balance signal that measures the transverse temperature difference across the sample.

In our case the temperature excursions, and hence the resistance changes in the thermometers, are small so that the output of very nonlinear sensors and a nonlinear bridge may be rationalized. Figure 2 shows the bridge circuit with  $r$  representing the ratio read from

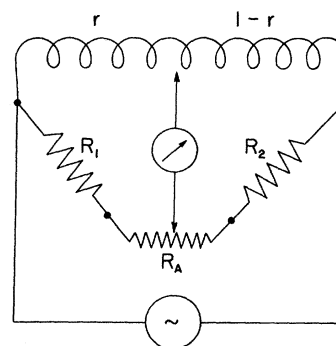


FIG. 2. ac bridge showing the two arms of the ratio standard,  $r$  and  $1-r$ ; the two differential thermometers,  $R_1$  and  $R_2$ ; the mismatch correction pot,  $R_A$ ; and the oscillator and detector.

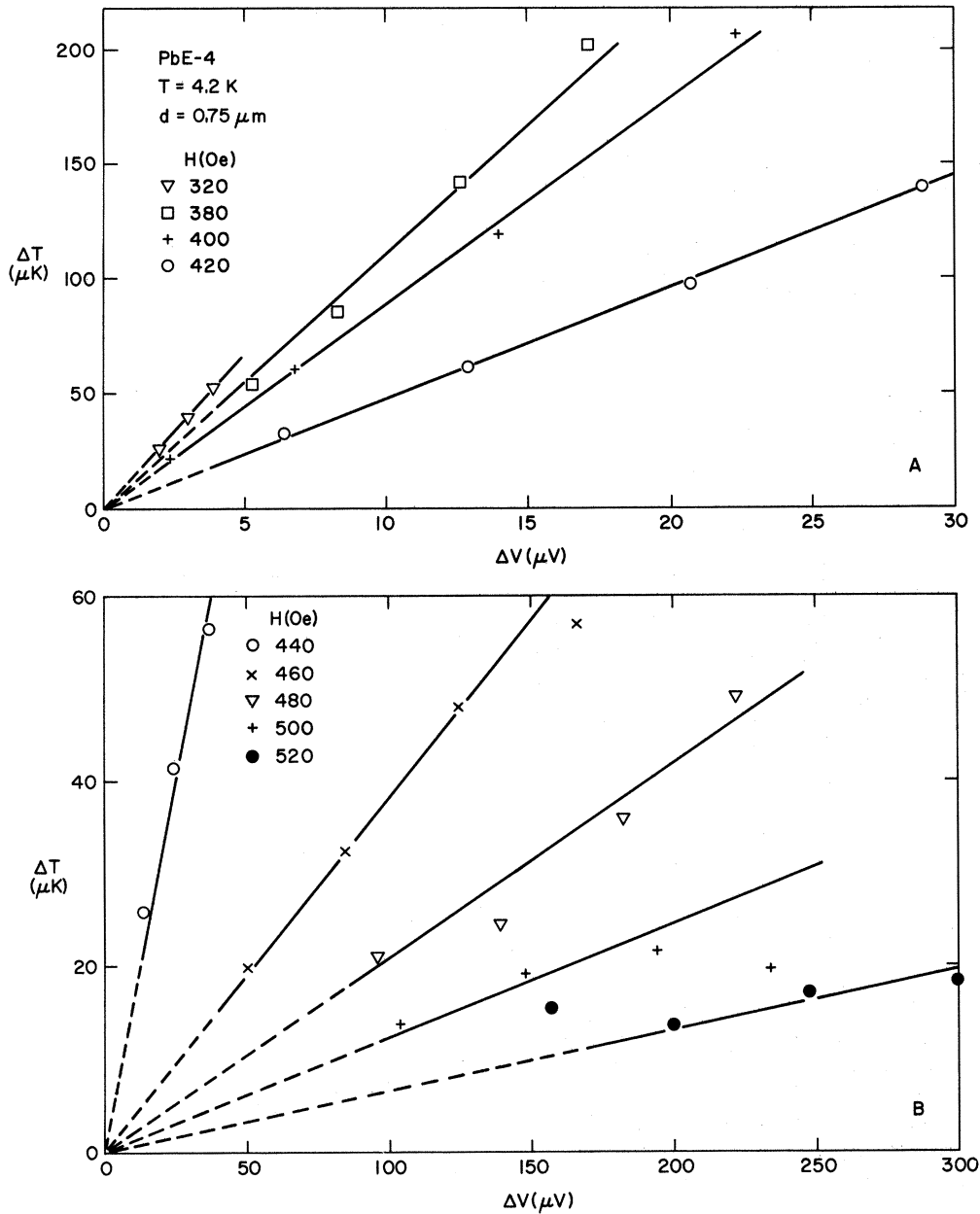


FIG. 3. Transverse temperature difference plotted versus longitudinal voltage difference for the  $0.75\text{-}\mu\text{m}$  Pb film at  $4.2\text{ K}$ . (a) Results for magnetic field values from 320 to 420 Oe. (b) Results for magnetic field values from 440 to 520 Oe.

the ratio transformer and  $R_1$  and  $R_2$  representing the two carbon thermometers.  $R_A$  is used to balance out the (small) mismatch in the  $4.2\text{ K}$  resistance of the thermometers. Over a small temperature range of, say,  $1\text{ K}$  near  $4.2\text{ K}$ , the temperature dependence of the resistance of the thermometer may be approximated by

$$1/T = A + B \ln R, \quad (1)$$

where  $A$  and  $B$  are determined for each thermometer by

calibrating relative to the vapor pressure of He and least-squares fitting to Eq. (1). If  $R_A$  is set to balance out the small  $4.2\text{-K}$  mismatch, then

$$1/T_1 - 1/T_2 = B \ln R_1/R_2, \quad (2)$$

where  $B$  is required to be similar in both sensors. Since  $T_1$  and  $T_2$  are nearly the same,

$$\Delta T \approx T^2 B \ln r / (1-r), \quad (3)$$

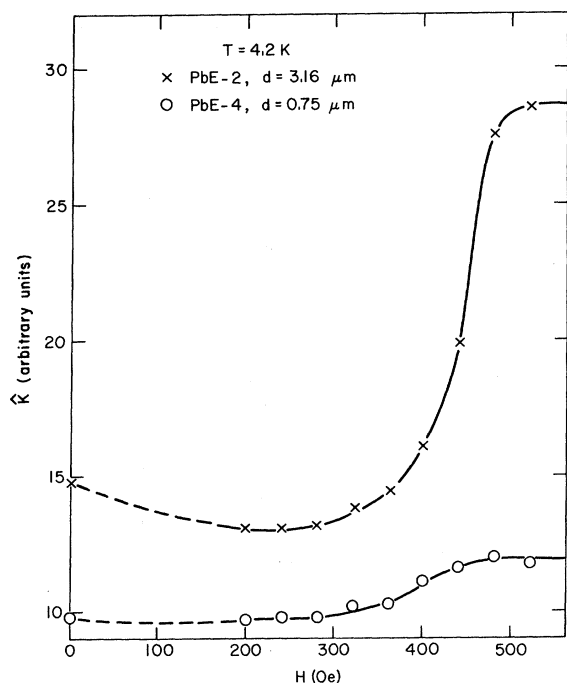


FIG. 4. Thermal conductance of the 3.16- $\mu\text{m}$  and 0.75- $\mu\text{m}$  Pb films at 4.2 K from 0 to 550 Oe applied magnetic field.

since at balance (see Fig. 2),

$$R_1/R_2 \approx r/(1-r). \quad (4)$$

Then the sensitivity of the differential thermometer may be defined as

$$d(\Delta T)/dr \approx T^2 B/(r-r^2), \quad (5)$$

which for our particular sensors works out to 60.8  $\mu\text{K}/0.00001$  ratio. In fact, this sensitivity is constant over the range of temperature differences encountered in the experiment. Since the noise level of the apparatus is on the order of a ratio difference of about 0.000001, the ultimate sensitivity to temperature differentials is about 6  $\mu\text{K}$  with a power dissipation on the order of  $10^{-12}$  W in the sensors.

### III. RESULTS AND DISCUSSION

Ettingshausen data were taken by halving the difference between the outputs from the thermometer bridge for currents flowing in both directions through the sample, thus eliminating the effect of Joule heating in the film which was on the order of 0.01 K in the worst case. Figure 3 shows the linear dependence of the transverse temperature difference on sample voltage at various magnetic fields for a 0.75- $\mu\text{m}$  Pb film.

The thermal conductance  $\hat{K}$  of the film-substrate assembly was determined as a function of magnetic field by plotting on the  $y$  axis of an  $x$ - $y$  recorder the temperature excursion of one of the thermometers

produced by heating one end of the sample, versus the heater voltage on the  $x$  axis. Then, by squaring the  $x$  coordinates of the 6-8 points generated, a straight line is obtained whose inverse slope, when divided by the heater resistance, is proportional to the rate of heat flow down the sample divided by the temperature gradient, i.e., proportional to

$$\hat{K} = \dot{Q}/\nabla_{\parallel} T.$$

Figure 4 shows  $\hat{K}$  for the two samples investigated as a function of applied magnetic field. From the Ettingshausen and heat-conductance measurements the entropy transported by the moving flux lines may be calculated. In the Ettingshausen experiment the rate of heat flow perpendicular to the transport current may be expressed as

$$\dot{Q}_{\perp} = A_f n S_{\phi} T v_{\phi}, \quad (6)$$

where  $A_f$  is the cross-sectional area of the film, i.e., the length between heat sinks times its thickness  $d$ ;  $n$  is the density of flux lines;  $S_{\phi}$  is the entropy per unit length and per unit flux;  $T$  is the absolute temperature;  $v_{\phi}$  is the flux flow velocity. Similarly, the rate of heat flowing in the thermal conductance experiment is

$$\dot{Q}_{\parallel} = K A \nabla_{\parallel} T,$$

where  $K$  is the effective thermal conductivity of the film substrate assembly and  $A$  is its "area." In this case  $A = t \times w$ , where  $t$  is the total thickness of film plus glass and  $w$  is the width of the specimen. Since  $n = B/\phi$ , where  $B$  is the magnetic field and  $\phi$  is the flux contained in a flux line and since no heat can flow in the perpendicular direction, we obtain the following with the help of Faraday's law:

$$\frac{S_{\phi}}{\phi} = \frac{10^{-1} L l}{2 d w^2 T R} \frac{V^2}{\Delta T_{\parallel}} \frac{\Delta T_{\perp}}{\Delta V_{\parallel}}, \quad (7)$$

where  $L$  is the distance between heater and heat sink,  $l$  is the distance between resistance probes,  $(V^2/\Delta T_{\parallel})$  is the slope of the straight lines obtained in the heat-conductivity experiment,  $(\Delta T_{\perp}/\Delta V_{\parallel})$  is the slope of the lines measured in the Ettingshausen experiment, and  $R$  is the heater resistance. Lengths are converted to cm,  $V$ 's to volts,  $R$  to ohms and  $T$ 's are in kelvins. With these units  $S_{\phi}/\phi$  is expressed in Oe/K.

As has previously been observed,<sup>11</sup> the thermal conductance passes through a minimum. The data plotted in Fig. 4 include the contribution of the glass substrate, but all the magnetic field dependence is assumed to be due to the films in the intermediate state.

Figure 5 shows the results of applying Eq. (7) to the Ettingshausen and thermal-conductance data taken on a 0.75- $\mu\text{m}$  film and a 3.16- $\mu\text{m}$  film together with some previously observed data for  $S_{\phi}/\phi$ .<sup>7</sup>

In Fig. 5 we compare the  $S_{\phi}/\phi$  results from three different methods of measurement for films of nearly the same thickness. The circles and squares represent the results of the present measurements of the Ettings-

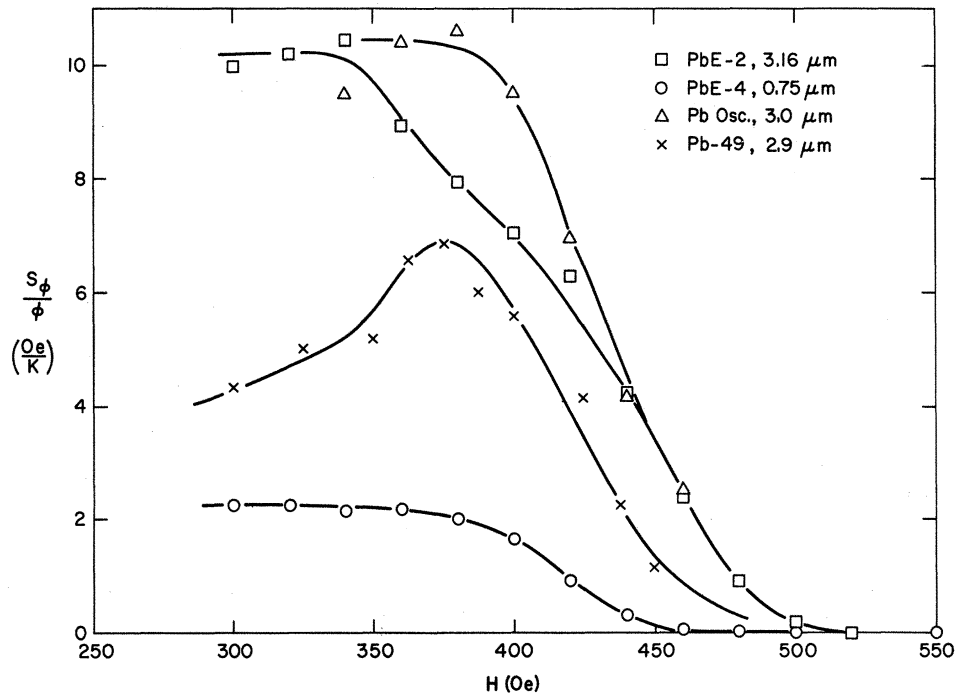


FIG. 5.  $S_\phi/\phi$ , the entropy per unit length and per flux, plotted versus applied magnetic field for the two samples investigated with the Ettingshausen effect (Pb E-2, Pb E-4) together with data obtained earlier from the Nernst effect with (Pb-Osc.) and without (Pb-49) an oscillatory magnetic field.

hausen effect. The triangles (Pb-Osc) show the results of an investigation of the Nernst effect, in which the influence of flux pinning was strongly reduced by the application of an oscillatory magnetic field oriented parallel to the static field.<sup>7</sup> The crosses (Pb-49) indicate earlier results obtained from the Nernst effect.<sup>7</sup> The Nernst effect measurement with an auxiliary ac field (Pb-OSC) and the present Ettingshausen effect measurements (Pb E-2) are seen to give similar results while the earlier Nernst effect measurements (Pb-49) produce somewhat diminished values. Using simple thermodynamic arguments, the quantity  $S_\phi/\phi$  is found from the difference of the entropy density in the normal and superconducting state as<sup>7</sup>

$$S_\phi/\phi = H_c(0)T/2\pi T_c^2,$$

where  $H_c(0)$  is the critical field at zero temperature and  $T_c$  the critical temperature. At 4.2 K this relation yields  $S_\phi/\phi = 10.4$  Oe/K. We note that samples Pb E-2 and Pb-Osc are in close agreement with this value at low magnetic fields. The previous Nernst effect results (Pb-49) show a decreasing  $S_\phi/\phi$  below 370 Oe. In the Nernst experiments severe flux pinning required the use of increasingly larger temperature gradients at lower magnetic fields. This disturbance of the sample may be responsible for the distorted  $S_\phi/\phi$  versus magnetic field data. A similar effect was observed in Sn and In films.<sup>8</sup>

Clem<sup>12</sup> and Maki<sup>13</sup> have discussed the transport

entropy of flux tubes in type-I superconductors. Clem postulates temperature gradients within the flux tubes due to their motion and shows such gradients to be responsible for reducing the transport entropy continuously to zero at  $H_c$ . However, his formulation also reduces the transport entropy at low magnetic fields from the value discussed above by a factor of  $(K_N - K_S)/K_N$ , where  $K_N$  and  $K_S$  are the thermal conductivity in the normal state and in the superconducting state, respectively. The present data are not consistent with such a reduction.

Maki assumes a laminar structure for the intermediate state with flux tubes moving along the edges of the laminae. From a time-dependent Ginzburg-Landau formulation, he extracts a value for  $S_\phi/\phi$  when  $B \ll H_c(T)$  and  $T < \frac{1}{3}T_c$ :

$$\begin{aligned} S_\phi/\phi &= [H_c(T)/4\pi T](1 + 1.33l/\xi_0) \\ &= 10.4(1 + 1.33l/\xi_0)\text{Oe/K} \end{aligned} \quad (8)$$

for Pb at 4.2 K. Here,  $l$  is the electronic mean free path and  $\xi_0$  the BCS coherence length. An analysis<sup>7</sup> of the resistance ratio versus thickness data taken on a large number of Pb films in this laboratory yields for Pb a  $\rho_0 l$  value of  $3.62 \times 10^{-11} \Omega \text{ cm}^2$ . The mean free paths at 4.2 K for the present samples are then 7.0  $\mu\text{m}$  for the 0.75- $\mu\text{m}$  film and 12.1  $\mu\text{m}$  for the 3.16- $\mu\text{m}$  film. Then  $l/\xi_0$  is of order  $10^2$  for our samples, since  $\xi_0$  is about

830 Å.<sup>14</sup> Apparently Maki's analysis in its present form does not apply to our films.

The observed dependence of the transport entropy on film thickness does seem to corroborate our earlier data. If indeed Pb at 4.2 K behaves like a type-II superconductor for films thinner than 1.5 μm, then it is not surprising that  $S_\varphi/\varphi$  is reduced. This behavior is likely attributable to the increased interactions between the closely spaced vortices.<sup>7</sup>

#### IV. CONCLUSIONS

The present experiments on the Ettingshausen effect confirm our earlier results from Nernst effect measurements that the transport entropy per unit length and per unit flux,  $S_\varphi/\varphi$ , decreases with decreasing film thickness below a critical thickness value. This behavior can be understood through the increasing vortex interaction in very thin type-I films. For the 3.16-μm film, sufficiently below  $H_c$ ,  $S_\varphi/\varphi$  is very close to the value calculated from simple thermodynamic arguments, whereas for the 0.75-μm film it is considerably reduced.

\* Based on work performed under the auspices of the U.S. Atomic Energy Commission.

- <sup>1</sup> Gordon Lasher, Phys. Rev. **154**, 345 (1967).
- <sup>2</sup> Kazumi Maki, Ann. Phys. (N.Y.) **34**, 363 (1965).
- <sup>3</sup> M. Tinkham, Phys. Rev. **129**, 2413 (1963).
- <sup>4</sup> G. D. Cody and R. E. Miller, Phys. Rev. **173**, 494 (1968).
- <sup>5</sup> G. D. Cody and R. E. Miller, Phys. Rev. **173**, 481 (1968).
- <sup>6</sup> J. A. Cape, Phys. Rev. **166**, 432 (1968).
- <sup>7</sup> R. P. Huebener and A. Seher, Phys. Rev. **181**, 710 (1969); R. P. Huebener and V. A. Rowe, Solid State Commun. **7**, 1763 (1969); V. A. Rowe and R. P. Huebener, Phys. Rev. **185**, 666 (1969).
- <sup>8</sup> P. R. Solomon and F. A. Otter, Jr., Phys. Rev. **164**, 608 (1967); P. R. Solomon, *ibid.* **179**, 475 (1969). Note that the correct spelling is Ettingshausen, and not Ettinghausen as appears in much of the literature.
- <sup>9</sup> Source: Division Lead Company, Summit, Ill.
- <sup>10</sup> Source: Emerson & Cuming, Inc., Canton, Mass.
- <sup>11</sup> K. Mendelssohn and J. L. Olsen, Proc. Phys. Soc. (London) **A63**, 2 (1950); Phys. Rev. **80**, 859 (1950); N. V. Zavaritskii, Zh. Eksperim. i Teor. Fiz. **38**, 1673 (1960) [Soviet Phys. JETP **11**, 1207 (1960)]; K. Mendelssohn and C. A. Shiffman, Proc. Roy. Soc. (London) **A255**, 199 (1960).
- <sup>12</sup> John R. Clem, Phys. Rev. **176**, 531 (1968); Phys. Rev. Letters **20**, 735 (1968).
- <sup>13</sup> Kazumi Maki, Progr. Theoret. Phys. (Kyoto) **42**, 448 (1969).
- <sup>14</sup> J. Bardeen and J. R. Schrieffer, *Progress in Low Temperature Physics*, edited by C. J. Gorter (North-Holland, Amsterdam, 1961), Vol. III, p. 243.

### rf-Induced Effects in Superconducting Tunnel Junctions\*

C. A. HAMILTON AND SIDNEY SHAPIRO

*Department of Electrical Engineering, University of Rochester, Rochester, New York 14627*

(Received 15 July 1970)

Arguments are presented to resolve experimental discrepancies with the theory of photon-assisted tunneling. A standing-wave model is suggested as a more realistic picture of the rf fields in a thin-film tunnel junction. By including the effects of this model in the theories of Tien and Gordon and of Werthamer, we obtain qualitative agreement with data on both the Josephson effects and the photon-assisted tunneling effects in the same junction. In an experiment with a junction sufficiently small to maintain a uniform rf field, we find excellent agreement with the unmodified theory. The low-frequency equivalence of the photon-assisted tunneling phenomenon and classical rf detection is also pointed out and used to demonstrate that the magnitude of the rf voltage appears correctly in the theory. We conclude that the Werthamer theory of rf-induced effects in superconducting tunnel junctions is on very firm experimental ground.

#### I. INTRODUCTION

It is well known that the current-voltage ( $I$ - $V$ ) characteristic of a superconducting tunnel junction is modified in the presence of an applied rf field. Constant-voltage steps arise from the interaction of the rf field with the ac Josephson current. In addition, the background curve is modified by a series of rounded steps caused by rf effects on the quasiparticle tunnel current. In this paper we present arguments to explain experimental discrepancies with the theory of the quasiparticle effects. Werthamer<sup>1</sup> has shown that the ac Josephson currents and the quasiparticle tunnel currents are intimately related in theory. We demonstrate this relationship experimentally and thus support our conclusions with data on both of these effects.

Observation of the quasiparticle steps, often called photon-assisted tunneling steps, was first reported by Dayem and Martin.<sup>2</sup> These steps in the  $I$ - $V$  curve are spaced at voltage intervals of  $hf/e$  up and down from the superconducting energy-gap voltage and may be thought of as arising from multiphoton emission and absorption processes. Each step is a sharp increase in current and has the same shape as the current increase at the energy-gap voltage  $2\Delta/e$  in the undisturbed  $I$ - $V$  curve. This phenomenon was first explained quantitatively by Tien and Gordon.<sup>3</sup> Their result is based on the assumption that the effect of the microwave field is a sinusoidal modulation of the bias voltage across the junction. Their analysis correctly predicts the voltages at which steps should appear and indicates that the